**INTERNATIONAL JOURNAL OF OPTIMIZATION IN CIVIL ENGINEERING**
***Int. J. Optim. Civil Eng., 2022; 12(1):15-32***

# OPTIMAL DESIGN OF DIAGRID MODULES BY PSEUDO-RANDOM DIRECTIONAL SEARCH

M. Shahrouzi[*, †] and A. Azizi
*Civil Engineering Department, Faculty of Engineering, Kharazmi University, Tehran, Iran*

## ABSTRACT

The present work reveals a problem formulation to minimize material consumption and improve efficiency of diagrids to resist equivalent wind loading. The integrated formulation includes not only sizing of structural members but also variation in geometry and topology of such a system. Particular encoding technique is offered to handle practical variation of diagrid modules. A variant of *Pseudo-random Directional Search* is utilized to solve this problem treating a number of three dimensional structural models. Several issues are investigated including the effect of variation in the building height, its aspect ratio and fixing or releasing diagrid angles. Consequently, especial trend of variation in diagrid angle is observed with superior structural responses with respect to sizing designs of the fixed-angle modules.

**Keywords:** tall building; structural design; non-uniform diagrid modules; layout optimization; pseudo-random directional search, swarm intelligence.

Received: 10 November 2021; Accepted: 12 January 2022

## 1. INTRODUCTION

Design of tall buildings under combined gravity and lateral loading is challenged by dimensions of available construction profiles to keep the storey sways within certain limits [1]. The matter has raised investigators to seek for more efficient lateral resisting systems [2,3]. Diagrid is one of the most recent developments in this field that consists of large-scale perimeter diagonals in addition to conventional frame members [4–6].

Systematic optimization should be employed in diagrid design instead of conventional

[*]Corresponding author: Civil Engineering Department, Faculty of Engineering, Kharazmi University, Tehran & Karaj, Iran
[†]E-mail address: shahruzi@khu.ac.ir (M. Shahrouzi)

trial and error due to very high cardinality of the search space in this problem. In the other hand, the constrained objective function is not usually analytical and it should be implicitly evaluated via structural analyses during optimization of tall buildings. Zero-order optimization methods are most suited for such a type of problem because they do not require any gradient information. Meta-heuristics fall in this category with several engineering applications [7–14]. Some popular algorithms can be referred as Ray Optimization [15], Opposition-Switching Search [16,17], Falcon Optimization Algorithm [18], Interactive Fuzzy Search [19], Coyote Optimization Algorithm [20], Water Evaporation Optimization [21], Salp Swarm Algorithm [22], Switching-Teams Algorithm [23], Heat Transfer Search [24], Plasma Generation Algorithm [25], Escaping Bird Search [26] and Water Strider Algorithm [27]. Several meta-heuristics have already been applied to structural problems [28] and MATLAB code of some recent ones can be found in [29].

The present work concerns the matter by formulating it as an optimization problem that allows even non-uniform diagrid angles for a perfect search toward the optimal design. An especial definition of design variables are employed so that both member sizing and geometry design of the diagrid modules can be simultaneously optimized.

The problem is then solved using two meta-heuristic algorithms in the category of directional search methods. As the first one, standard *particle swarm optimizer*, PSO, is employed. For the second, a simplified *Pseudo-random Directional Search*, PDS, is utilized for this problem. The proposed method is selected in this study as it takes merit of indirect information share in Ant Colony Optimization [30], stochastic selection of Genetic Algorithms [31] and vector-based search in PSO [32]. Performance of PDS is further evaluated in optimal sizing and layout design of diagrid systems.

## 2. FORMULATION OF OPTIMAL DESIGN PROBLEM

In the present optimal design of tall building with diagrid system, it is desired to minimize the material consumption provided that the design code requirements for stress and deflection are satisfied. Member sizing and diagrid layout are simultaneously altered via the following problem formulation to obtain the lightest feasible structure.

$$\begin{aligned} &\textit{Minimize} \quad W(\underline{X}) = \rho \sum_{i=1}^{Ng} \sum_{j=1}^{Nm(i)} L_i A_i \\ &\textit{Subject to} \\ &\qquad x_i^{LB} \le x_i \le x_i^{UB}, \quad i = 1,...,N_d \\ &\qquad g_j(\underline{X}) \le 0 \quad , \quad j = 1,...,N_c \end{aligned} \tag{1}$$

According to Eq.(1) the side constraints are distinguished from the behavioral ones because they undergo different treatment during optimization. For the first case, when a sizing variable falls outside of its allowable bounds it is substituted with the nearest limit. However, violation of behavioral constraints is treated by a penalty function as:

$$Minimize\ f = W(X) \times (1 + K_P \sum_j \max(0, g_j(\underline{X}))^2) \quad (2)$$

The first term in Eq. (2) denotes total weight of a structure with the $i^{th}$-member's length of $L_i$ and cross sectional area of $A_i$ where $\rho$ stands for the material density. The second term of Eq.(2) applies penalty for every $j^{th}$ behavioral constraint that was denoted by $g_j(\underline{X}) \le 0$ in Eq.(1). A penalty constant $K_p$ is prescribed prior to running the algorithm. Behavioral constraints include design-code requirements for the resulted stress and displacement responses due to *Iranian National Building Code*: *Part 10* [33]. They are normalized to the allowable limits on story sways and member stresses, respectively.

In the problem formulation of Eq. (1), the design vector is structured as in $\underline{X} = < \underline{S}, \underline{Z} >^T$. It not only includes section indices by $\underline{S} = < s_1, ..., s_m >$ to be associated for structural members but also governs geometrical/topological part of design using $\underline{Z} = < z_1, ..., z_n >$. According to the present encoding method, every such $z_k$ denotes the number of frame stories covered by the $k^{th}$ diagrid module where $k$ is numbered from the lowest module to the highest among the structural height.

## 3. APPLIED OPTIMIZATION ALGORITHMS

Several meta-heuristic algorithms have already been introduced to solve engineering optimization problems. Majority of them apply graduate improvement of a current search candidate via the following typical relation:

$$\underline{X}^{k+1} = \underline{X}^k + \underline{V}^{k+1} \quad (3)$$

$\underline{X}^{k+1}$ and $\underline{X}^k$ are the design vectors at the current ($k$+1) and previous ($k$) iterations of the main algorithm, respectively. The present work concerns two algorithms in this class of search methods with different procedures in calculating $\underline{V}^{k+1}$; i.e. the velocity vector. Both these algorithms are initiated with a random population of particles provided that every individual falls within lower and upper bounds of the design vector.

### *3.1 Particle Swarm Optimization*

The *Particle Swarm Optimization*, PSO, is a population-based meta-heuristic inspired by swarm intelligence of bird flocks [32]. Every artificial bird or particle denotes a candidate solution which takes the corresponding value of the design variables as its position vector. In order to update the position of the $i^{th}$ bird in the $k^{th}$ iteration, PSO applies the following formula.

$$\underline{V}_i^{k+1} = c_i \underline{V}_i^k + rand \times c_c \times (\underline{P}_i^k - \underline{X}_i^k) + rand \times c_s \times (\underline{B}^k - \underline{X}_i^k) \quad (4)$$

There are three terms in Eq. (4) described as:

- Inertial term: moving in the same direction of the previous movement .
- Cognitive term, in which a particle uses its best experience up to the current iteration. Such a position is denoted by $\underline{P}_i^k$ or the $i^{\text{th}}$ particle in the population.
- Social term: simulates moving toward $\underline{B}^k$; i.e. the global best position among all the particles up to the current iteration.

In Eq. (4), $c_i, c_c, c_s$ stand for the prescribed inertial, cognitive and social coefficients, respectively and *rand* function generates uniform random numbers between 0 and 1.

At every iteration, the new position of an $i^{\text{th}}$ particle is updated by Eq. (3) and Eq. (4). It is accomplished for all the particles and the procedure is repeated for a prescribed number of iterations. The global best vector at the final iteration is announced as the optimal solution. PSO is in fact a directional search which applies new velocity for each particle by vector-sum of Eq. (4) in any walk in the design space.

### *3.2 Pseudo-random Directional Search*

Another way of generating new solutions, is to select only one direction at a walk step, instead of applying vector-sum of such terms. It is utilized in *Pseudo-random Directional Search*, PDS [34]. This hybrid method mimics indirect share of experienced information from *Ant Colony Optimization* [30]. PDS allows each particle to make any its walk at a distinct direction among the prescribed movement terms in the algorithm.

A variant of PDS is introduced here with fewer parameters to be tuned for practical design. In this method, position of any $i^{\text{th}}$ particle at $k^{\text{th}}$ iteration is updated by Eq. (3); where its velocity is governed by the following formula.

$$\underline{V}_i^{k+1} = 2 \times rand \times (\underline{S}_j^k - \underline{X}_i^k) \tag{5}$$

The term $\underline{S}_j$ in PDS terminology is called the $j^{\text{th}}$ state. In the present work, it is selected among the prescribed set of states $< \underline{X}_i^k + \underline{V}_i^k,\ \underline{P}_i^k\ ,\underline{B}^k\ ,\ \underline{R}_i^k >$. $\underline{R}_i^k$ denotes a random particle in the current population. Note that for each of these states, its position and value may vary for different iterations and particles. Every $i^{\text{th}}$ particle, selects its state number, *j*, as an integer from the set $< 1, 2, 3, 4 >$ using the following relation.

$$j = \begin{cases} \arg\max_l (P_{i,l}) & if \quad r \le q_0 \\ j^P & if \quad q_0 < r \le q_1 \\ j^R & otherwise \end{cases} \tag{6}$$

in which, $q_0$, $q_1$ are positive control parameters and $r = rand$ . $j^P$ denotes a state number resulted from a *Roulette Wheel Selection* procedure using such probability values. $P_{i,l}$ is a probability measure for choosing the $l^{\text{th}}$ state by the $i^{\text{th}}$ particle. It is calculated as:

Table 1: Pseudo-code of the utilized PDS

- *Set control parameters:* $PopSize, N_{\max}, \ q_0, q_1, \alpha$
- *Randomly generate the 1st population and their velocities, set* $k = 1$
- *Initiate pheromone matrix*
- *Repeat while* $k \le N_{\max}$
  - *Evaluate fitness for all particles and determine* $\underline{P}_i^k, \underline{B}^k, \underline{R}_i^k$
  - *Repeat for each particle* $i = 1$ *to* $PopSize$

    *% determine* $j \in \{1,2,3,4\}$ *and* $\underline{S}_j^k \in \{\underline{X}_i^k + \underline{V}_i^k, \underline{P}_i^k, \underline{B}^k, \underline{R}_i^k\}$ *by:*
    - $r = rand$
    - *If* $r > q_1$ *then randomly choose one state to move:* $j = randi(4)$
    - *else calculate* $P_{i,l}$ *based on existing pheromone*
      - *if* $q_0 < r \le q_1$ *then determine* $j$ *by Roulette Wheel selection using* $P_{i,l}$
      - *else* $j$ *corresponds the state* $\underline{S}_j^k$ *which has the maximum* $P_{i,l}$
      - *end if*
    - *end if*
    - *update velocity of particle:* $\underline{V}_i^{k+1} = 2 \times rand \times (\underline{S}_j^k - \underline{X}_i^k)$
    - *move* $\underline{X}_i^{k+1} = \underline{X}_i^k + \underline{V}_i^{k+1}$
  - *end for*
  - *Update pheromone* $\tau_{i,j}^{(k+1)}$ *for every* $i, j$ *by*
    - $\tau_{i,j}^{(k+1)} = (1-\alpha) \times (\tau_{i,j}^{(k)} + \alpha)$
    - $\tau_{i,j}^{(k)} = \begin{cases} \dfrac{\tau_{i,j}^{(k)}}{\min_h (\tau_{i,h}^{(k)})} & if \quad \min_h (\tau_{i,h}^{(k)}) \ge 1.5\alpha \\ 1 & otherwise \end{cases}$
  - *end for*
- $k = k + 1$
- *end while*
- *Announce* $\underline{X}^* = \underline{B}^k$

$$P_{i,l} = \frac{\tau_{i,l}}{\sum_{h=1}^{NumStates} \tau_{i,h}} \tag{7}$$

$\tau_{i,h}$ denotes the existing amount of pheromone on the edge connecting the particle $i$ to the state $h$ in an abstract graph [34]. The algorithm uses indirect information share by pheromone deposition and evaporation due to the following relation.

$$\tau_{i,j}{}^{(k+1)} = (1-\alpha)\times(\tau_{i,j}{}^{(k)} + \alpha) \tag{8}$$

Both the evaporation and deposit ratios are implemented here by $\alpha$ . The pheromone matrix$\left[\tau_{i,j}\right]$is initiated with 0 at diagonals and 1 at the other components. During the optimization, this matrix is reinitiated when the minimum pheromone falls below a threshold; which is taken $1.5\alpha$ in the current study. The algorithm is started with *PopSize* number of particles and is repeated for $N_{\max}$ iterations. Pseudo-code of this PDS algorithm is given in Table 1. It is worth notifying that the proposed variant of PDS uses the same number of control parameters as PSO.

## 4. NUMERICAL SIMULATION

Performance of the aforementioned algorithms in the optimal design of diagrid system is evaluated treating a number of structural models under gravitational and wind loading. Table 2 gives general definition and notation of the treated models. Material properties are reported in Table 3. Typical story length is 3.00*m* while every bay has a length of 4.00*m* in each direction.

Table 2: General characteristics of the treated models

| Model ID | Number of stories | Number of bays in X direction | Number of bays in Y direction | Aspect ratio |
|---|---|---|---|---|
| **20s1** | 20 | 6 | 6 | 1.0 |
| **30s1** | 30 | 6 | 6 | 1.0 |
| **20s2** | 20 | 8 | 4 | 2.0 |

Table 3: Properties of constructional steel material

| Grade | Density $\rho(kgf/m^3)$ | Poisson ratio $\upsilon$ | Stiffness modulus $E(kgf/m^2)$ | Yield stress $Fy(kgf/m^2)$ |
|---|---|---|---|---|
| **St-37** | 7850 | 0.3 | $2.1*10^{10}$ | $2.4*10^{7}$ |

It is assumed that interior beam-column joints in the structure are hinged and lateral load resistant system is attached on perimeter frames. A dead load of DL=600*kgf/m*$^2$ and a live load of LL=200*kgf/m*$^2$ is distributed at any floor and further implemented in the following load combinations:

$$
\begin{aligned}
&1)\ DL \\
&2)\ DL + LL \\
&3)\ DL \pm 0.84WL_x \\
&4)\ DL \pm 0.84WL_y \\
&5)\ DL + 0.75(LL \pm 0.84WL_x) \\
&6)\ DL + 0.75(LL \pm 0.84WL_y)
\end{aligned}
\tag{9}
$$

The wind loads $WL$ are calculated due to *Iranian National Building Code: Parts 6* [35] for a base wind speed of 130*km/h*. Fig. 1 shows sample wind profile among the building height. According to the employed design code, maximum drift ratio should not exceed (H/500) where "H" is entire height of the structure over its base.

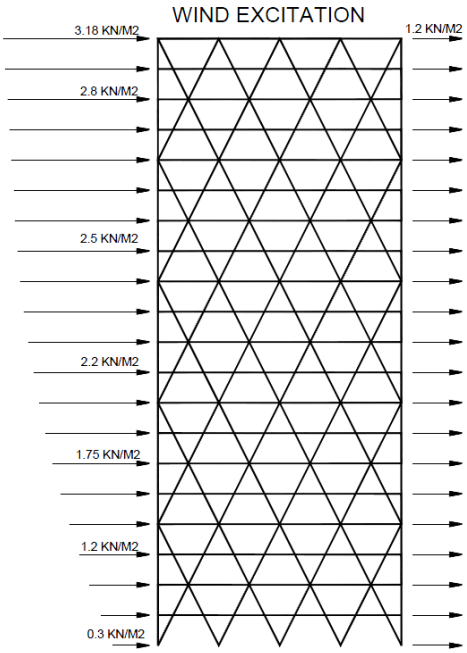


Figure 1. Windward and leeward profile of wind pressure on a typical 20-storey diagrid model (due to Iranian National Building Code [35])

Table 4: Applied control parameters of PSO

| *PopSize* | $N_{\max}$ | $c_i$ | $c_c$ | $c_s$ |
|---|---|---|---|---|
| 11 | 250 | 0.9 to 0.1 | 2.1 | 1.9 |

Table 5: Applied control parameters of PDS

| *PopSize* | $N_{\max}$ | $q_0$ | $q_1$ | $\alpha$ |
|---|---|---|---|---|
| 11 | 250 | 0.3 | 0.9 | 0.1 |

Optimization parameters for each example are tuned and the results are derived using several trial runs. Table 4 reports 5 control parameters of PSO. Note that tuned values for cognitive and social coefficients in PSO are almost 2 while the inertial coefficient is linearly decreased from 0.9 to 0.1 during iterations of the algorithm. According to Table 5, the proposed PDS is run with two general and three specific control parameters. The general parameters; i.e. population size and number of iterations are taken identical with PSO.

Structural members are symmetrically divided into three groups: beams, columns and diagrid bracings. For each group 16 sections are available to be selected during the optimization. For example; there are $16^{10}$ alternatives for designing the 20s1 model that means a quite large search space.

A number of issues are then investigated including the effect of variation in height, the type of design variables and uniformity of diagrid angles. For the latter case, two types of optimization are implemented: in the 1st type, diagrid angles are kept fixed while in the 2nd, they are released so that non-uniform modules can arise in the optimal design.

### *4.1 Performance evaluation in simultaneous size and layout optimization*

As the 1st example, 20s1 model is treated by PSO and PDS using the problem formulation of Eq. (1). Convergence history of the best result in Fig. 2, shows superior efficiency and effectiveness of PDS over PSO. Furthermore, a statistical study is performed by several independent runs leading to the results of Table 6. It confirms that PDS has obtained the least weight among the best results; however, it has been almost similar to PSO in the mean and worst results in this example.

Fig. 3 shows that both the methods have resulted in non-uniform diagrid angles among the structures' height. It may be noticed that such a variation in diagrid angles is smoother in the result of PDS than that of PSO.

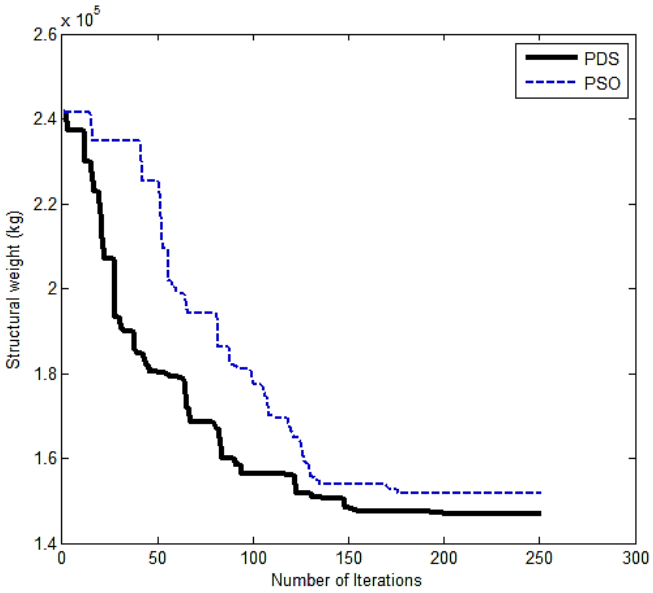


Figure 2. Comparison of convergence histories for the optimal design of 20s1

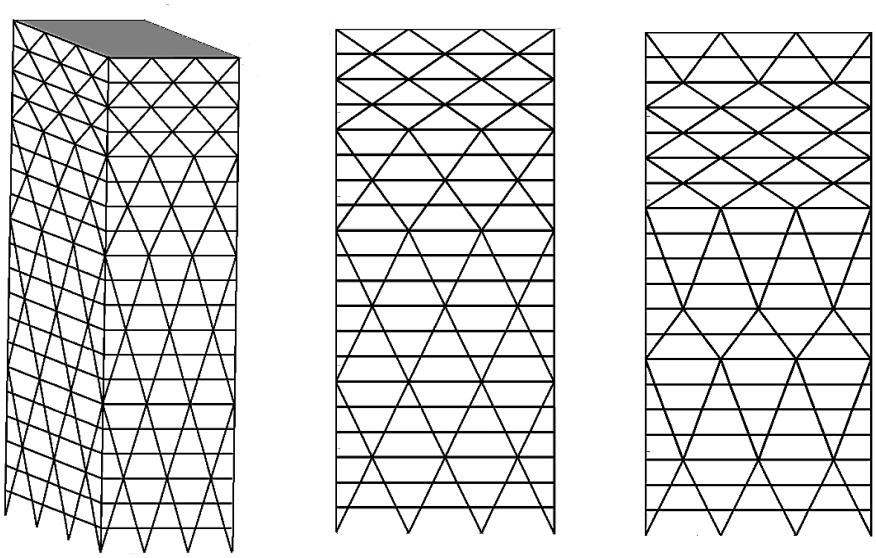

(a) (b) (c)

Figure 3. Non-uniform optimal diagrid layouts of 20s1 by (a),(b) PDS and (c) PSO

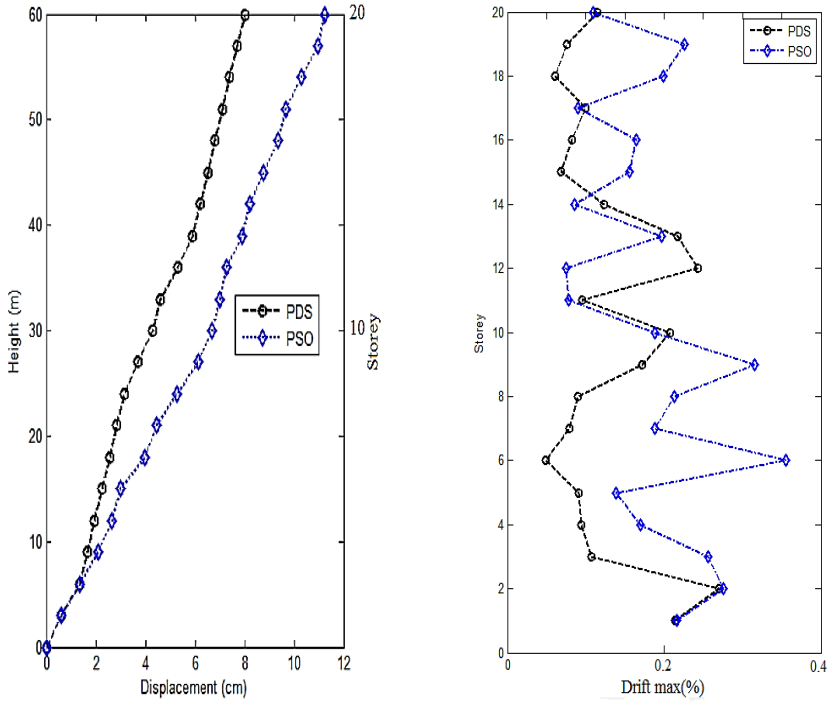


(a) (b)

Figure 4. Comparison of structural responses in (a) displacements and (b) drift ratios for the optimal design of 20s1 example with non-uniform modules

Table 6: Results of structural weight ($10^3$kg) for 20s1 model

| Method | Best | Worst | Mean |
|---|---|---|---|
| **PSO** | 154 | 170 | 162 |
| **PDS** | 148 | 172 | 162 |

The employed algorithms are compared in Fig. 4 regarding structural responses for the optimal designs of 20s1 model. It is evident that PDS has led to lower story sways than PSO. In its best design, PSO has resulted in maximum drift ratio of 0.37% and the corresponding roof displacement of 11.2*cm*. Applying PDS; such responses are reduced to 0.27% and 8.0*cm*, respectively. Note that these results are obtained even with lower consumption of structural material. It confirms superior performance of PDS over PSO; not only in weight minimization but also in reduction of absolute and relative structural deflections.

*4.2 Effect of variation in the building height*

The previous test is repeated for 30s1 model to study effect of variation in the building's height. In this example, the number of symmetric groups for beams, columns and braces are 20, 15 and 15, respectively. Statistical results are derived for simultaneous size and geometry optimization as reported in Table 7. It can be realized that for this taller example, PDS superiority over PSO has been extended from the best result to the mean and worst results of the structural weight among several independent runs. The matter is confirmed via comparison of convergence histories for the best results in Fig. 5. Trend of result improvement shows that despite PSO, the employed PDS has not led to premature convergence. In another word, PDS has exhibited better global search capability than PSO toward high quality solutions.

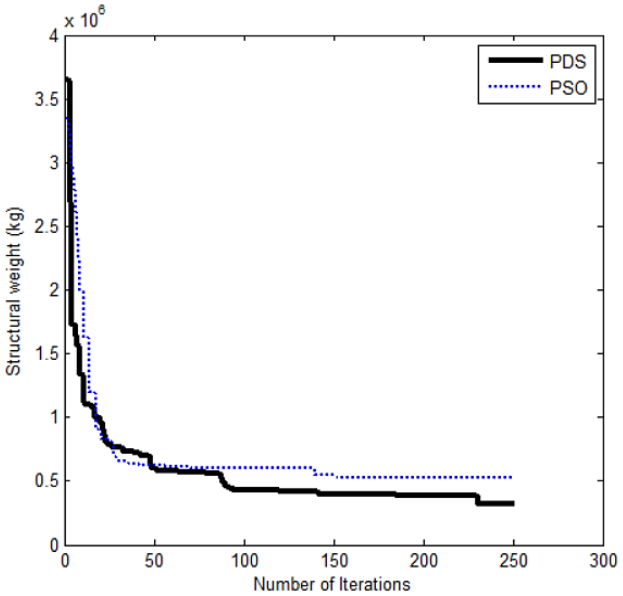


Figure 5. Comparison of convergence histories for the optimal design of 30s1

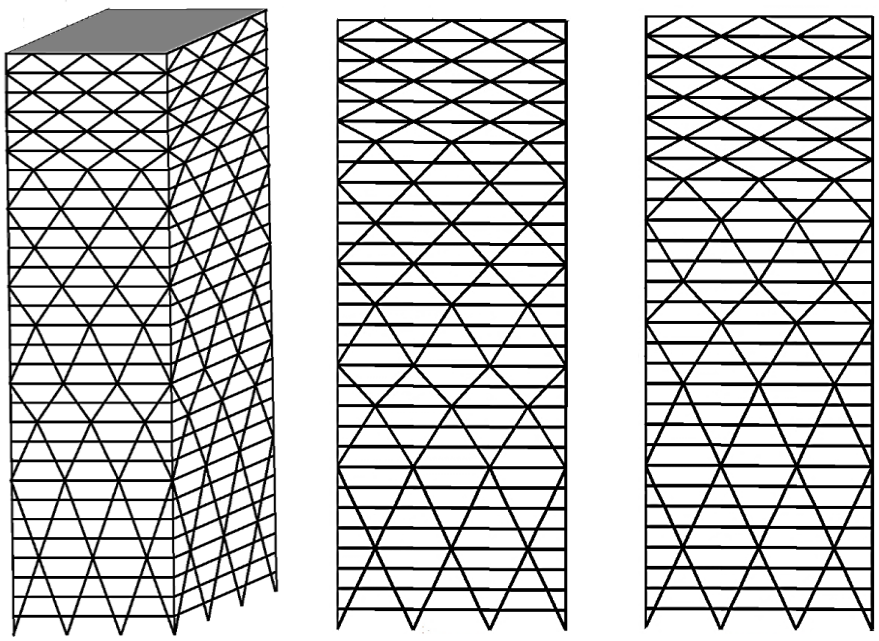

(a) (b) (c)

Figure 6. Non-uniform optimal diagrid layouts of 30s1 by (a),(b) PDS and (c) PSO

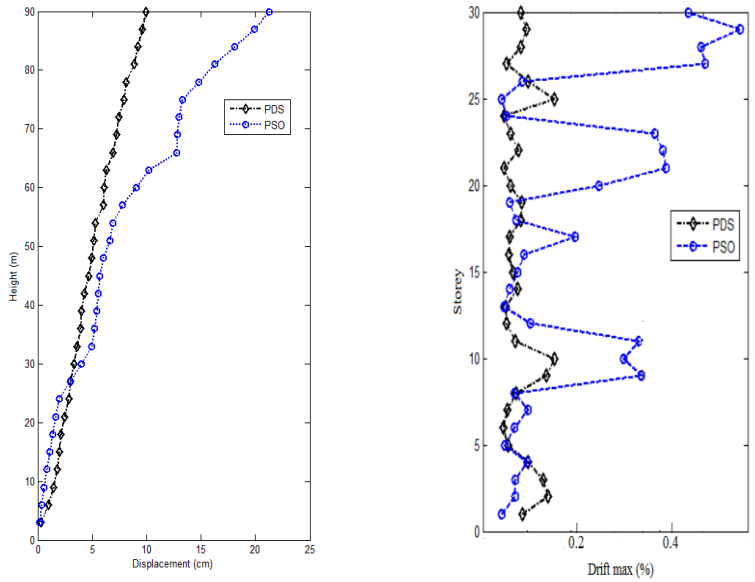


(a) (b)

Figure 7. Comparison of structural responses in (a) displacements and (b) drift ratios for the optimal design of 30s1 example and (c) PSO

Trend of variation in the diagrid-angle with height is better declared for this taller example in Fig. 6. In such optimal layouts the diagrid angle with the horizontal direction

decreases for the upper stories where modules distribution become denser in order to withstand story sways.

Table 7: Results of structural weight ($10^3$kg) for 30s1 model

| Method | Best | Worst | Mean |
|---|---|---|---|
| **PSO** | 538 | 597 | 550 |
| **PDS** | 326 | 410 | 369 |

Comparison of structural responses in Fig. 7 declares that PDS has resulted in much more uniform inter-story drifts than PSO. Maximum drift values obtained by PDS and PSO are 0.18% and 0.57% while corresponding lateral displacements are 9.9*cm* and 21.7*cm*, respectively. Such a difference is more considerable in this taller building with respect to the previous example; especially near the roof. At such higher levels, the rate of increasing storey drifts in PSO design has drastically changed while the PDS design has a uniform rate of drift variation. Note that such higher rate via PSO design means irregularity in height-wise stiffness distribution. It may correspond localized soft storey effect that is not desired in structural design.

*4.3 Effect of releasing modules uniformity in optimization*

The 20s1 model is re-treated here with another type of optimization; that is structural sizing with constant diagrid-angles merely resulting in uniform modules. It is obtained by excluding the geometrical part $< z_k >$ from design vector in Eq. (1). Fig. 8 compares PDS designs via the aforementioned cases of diagrid optimizations; first with uniform modules and second when such uniformity is released. For the sake of true comparison, the number of diagrid modules is kept constant.

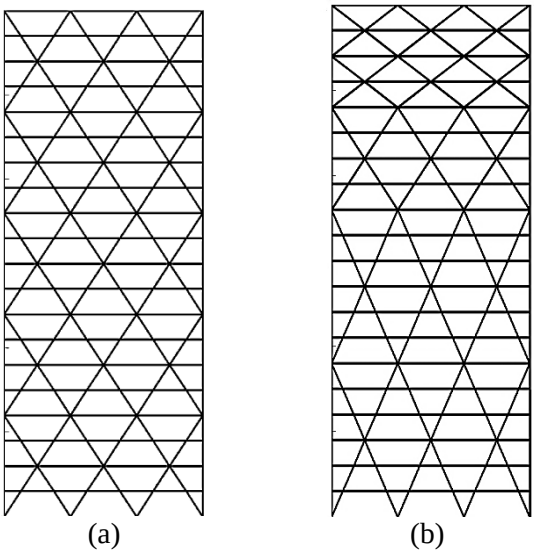

(a) (b)

Figure 8. Results of PDS for 20s1 in (a) uniform and (b) non-uniform diagrid design

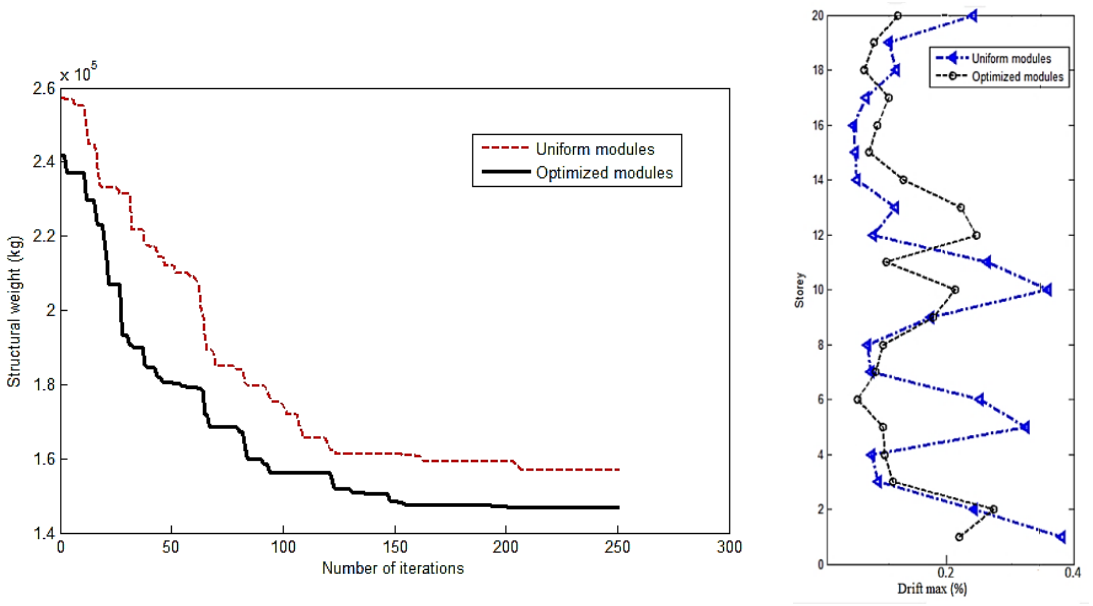


(a) (b)

Figure 9. Comparison between uniform and non-uniform diagrid optimization regarding (a) trend of weight minimization and (b) storey drift profile at the final design

In the first case, only sizing optimization is performed for the model and diagrid angle is fixed. But in the second case, both layout and sizing is optimized. Although, the second case has resulted in non-uniform modules, a uniform trend of decreasing diagrid angle is observed from the base to the roof level.

Fig. 9a shows that the optimized non-uniform module design has been superior in minimizing structural weight provided that all the code-based stress and deflection constraints are met. According to Fig. 9b, non-uniform design of diagrid has resulted in lower story drifts regarding the maximal response even with less structural weight than the design with uniform modules. It can also be noted that the trend of drift variation with the building height is smoother for the optimized non-uniform diagrid. The matter confirms necessity of releasing diagrid angles during optimization and its better structural responses in addition to providing benefit of lower steel consumption.

### *4.4 Effect of variation in aspect ratio of the building plan*

In order to illustrate performance of the proposed method in the buildings with non-square plans, the 20s2 model is treated. In this example, the longitude-to-transverse aspect ratio is taken 2 times of that in the 20s1 model.

The best optimal layouts obtained by PSO and PDS are depicted in Fig. 10. These results are different from previous examples regarding that the number of diagrid modules in longitude direction is twice that in the transverse width of this building. However, the trend of height-wise variation in diagrid angle is similar to the square plan examples; that is decreasing such angle as the story level increases.

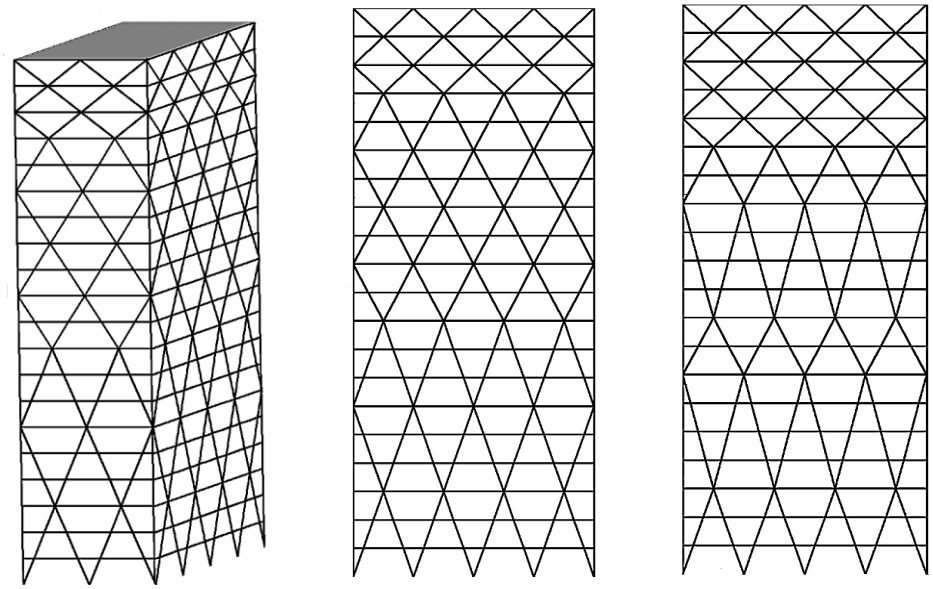

(a) (b) (c)

Figure 10. Non-uniform optimal diagrid layouts of 20s2 by (a),(b) PDS and (c) PSO

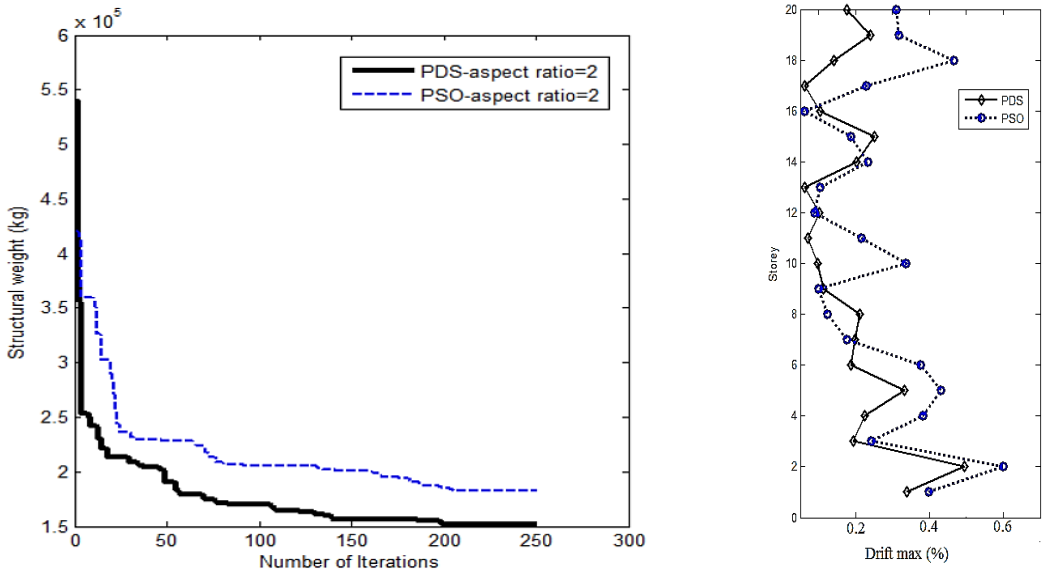


(a) (b)

Figure 11. (a) Convergence history and (b) storey drift profile at the final design for 20s2

According to Table 8 and Fig. 11a, PDS has achieved better structural weights than PSO, not only in its best run but also regarding the mean and worst results. In comparison with Fig. 2, such a weight difference is considerably higher than those obtained for square-plan model of the 1st example. In another word superiority of PDS over PSO is more declared for the greater aspect ratio in 20s2 model.

Table 8: Results of structural weight ($10^3$kg) for 20s2 model

| Method | Best | Worst | Mean |
|---|---|---|---|
| **PSO** | 178 | 191 | 183 |
| **PDS** | 153 | 184 | 168 |

Such superiority is shown in Fig. 11b from another point of view; that is lower amount of drift ratios obtained by PDS than PSO in most of the story levels. However, marginal drift values for this example with the aspect ratio of 2 are greater than those for optimal design of the 1st example with square plan. Critical drift and displacement responses in the PSO design of this example are 0.62% and 15.7 cm, respectively. PDS has considerably reduced these values to 0.51% and 10.9 cm.

According to Fig.12, it can be realized that in the same iteration, the number of over-stressed members in PDS design has been fewer than PSO. In another word, PDS has performed betted in avoiding undesired stress concentration even with its less consumption of structural material with respect to PSO. It is important for practical design of diagrid system due to code based requirements.

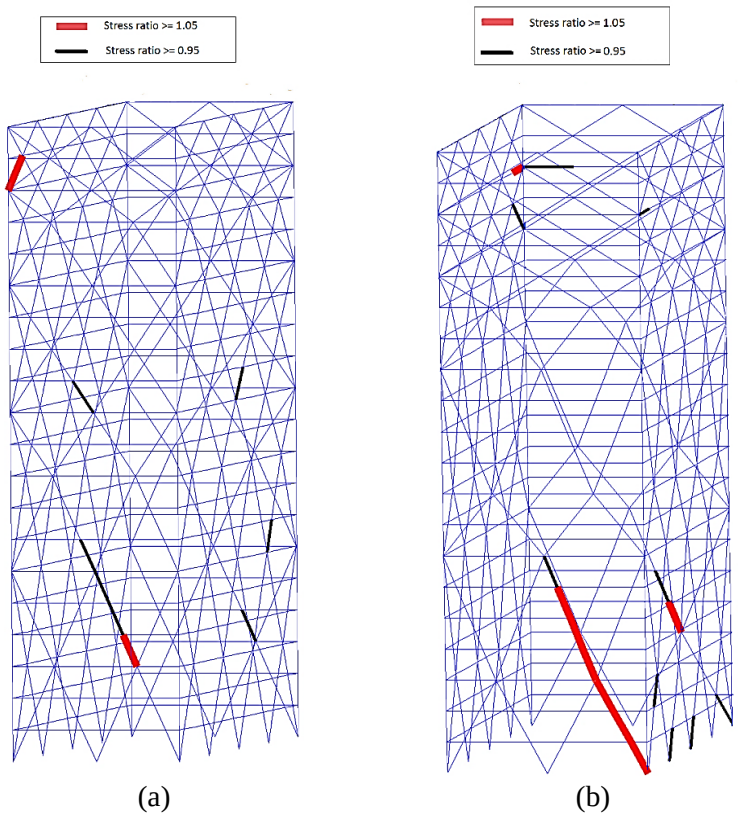


(a) (b)

Figure 12. Distribution of overstressed members in the optimal design of 20s2 diagrid model by (a) PDS and (b) PSO

## 5. CONCLUSION

Optimal design of diagrid systems was assessed within two types of formulations. In the first type only size of structural members are taken as design variables while in the second, both sizing and layout variables are taken into account using an especial decoding to practical position of diagrid nodes.

For practical purposes, the number of control parameters in the proposed variant of PDS is lowered as few as PSO. Nevertheless, higher quality of solutions by the proposed PDS showed it can be better tuned than popular PSO to overpass local optima in the treated examples.

It was declared that optimal designs of the 2nd problem include non-uniform modules of diagrid system. In another experiment using sizing-only formulation, the non-uniform layouts revealed lower optimal weights than the uniform layouts with the same number of diagrid modules. Meanwhile, the optimal non-uniform designs could better reduce the story sways against static wind loads satisfying codified stress and deflection requirements. Hence, the 2nd formulation is superior to the sizing-only design due to its freedom in spatial distribution of diagrid modules.

It is observed that in a proper optimal design, diagrid modules are usually non-uniform and become denser in the upper stories in order to provide sufficient stiffness against lateral loads to control consequent drifts. In the light of the present study, the angle of diagrid modules with the horizon is recommended to be reduced in higher levels so that every upper module covers fewer stories.

## REFERENCES

1. Hasançebi O, Çarbas S. Ant colony search method in practical structural optimization, *Int J Optim Civil Eng* 2011; **1**: 91–105.
2. Ali MM, Moon KS. Structural developments in tall buildings: current trends and future prospects, *Archit Sci Rev* 2007; **50**: 205–23.
3. Panchal NB, Patel VR. Diagrid structural system: strategies to reduce lateral forces on high-rise buildings, *Int J Res Eng Technol* 2014; **03**: 374–8.
4. Moon KS. Optimal grid geometry of diagrid structures for tall buildings, *Archit Sci Rev* 2008; **51**: 239–51.
5. Shahrouzi M, Meshkat-dini A, Azizi A. Optimal wind resistant design of tall buildings utilizing mine blast algorithm, *Int J Optim Civil Eng* 2014; **5**: 137–50.
6. Shahrouzi M, Azizi A. Configuration design of diagrids via module-based optimisation by an enhanced meta-heuristic algorithm, 5th International Conference Soft Computing Optimization Civil, Structure and Environment Engineering, Lake Garda, Italy: Elsevier, 2019.
7. Kaveh A, Ilchi Ghazaan M. *Meta-Heuristic Algorithms for Optimal Design of Real-Size Structures*, Springer International Publishing, 2018.
8. Shahrouzi M, Ojani A. Seismic performance of optimal steel moment frames with variation of design load patterns, *Comput Res Prog Appl Sci Eng* 2018; **04**: 19–26.

9. Bäck T, Eiben AE, Van der Vaart NAL, Binitha S, Sathya SS. A survey of bio inspired optimization algorithms, *Int J Soft Comput Eng* 2012; **2**: 137–51. doi:10.1007/b100601.
10. Yang X, Gandomi AH, Talatahari S, Alavi AH. *Metaheuristics in Water Resources, Geotechnical and Transportation Engineering*, Wltham, MA, USA, Elsevier Inc, 1st ed, 2012; **136**.
11. Kaveh A. *Applications of Metaheuristic Optimization Algorithms in Civil Engineering*, Switzerland: Springer International Publishing; 2017.
12. Degertekin SO, Lamberti L, Ugur IB. Sizing, layout and topology design optimization of truss structures using the Jaya algorithm, *Appl Soft Comput J* 2018; **70**: 903–28.
13. Kaveh A, Biabani Hamedani K, Milad Hosseini S, Bakhshpoori T. Optimal design of planar steel frame structures utilizing meta-heuristic optimization algorithms, *Struct* 2020; **25**: 335–46.
14. Geem ZW, Sim KB. Parameter-setting-free harmony search algorithm, *Appl Math Comput* 2010; **217**: 3881-9.
15. Kaveh A, Khayatazad M. Ray optimization for size and shape optimization of truss structures, *Comput Struct* 2013; **117**: 82–94.
16. Shahrouzi M. Optimal spectral matching of strong ground motion by opposition-switching search. EngOpt 2018 Proceedings of the 6th International Conference Engineering Optimization, Lisbon, Purtugal: Springer International Publishing; 2018, pp. 713–724.
17. Shahrouzi M, Salehi A. Design of large-scale structures by an enhanced metaheuristic utilizing opposition-based learning, 2020 4th Conference on Swarm Intelligence and Evolutionary Computation (CSIEC), IEEE; 2020, pp. 27–31.
18. Hochsteiner E, Mariani VC, Coelho L dos S. Design of heat exchangers using Falcon Optimization Algorithm, *Appl Therm Eng* 2019; **156**: 119–44. doi:10.1016/j.applthermaleng.2019.04.038.
19. Mortazavi A. Interactive fuzzy search algorithm: A new self-adaptive hybrid optimization algorithm, *Eng Appl Artif Intell* 2019; **81**: 270–82.
20. Pierezan J, Coelho L. Coyote Optimization Algorithm: A New Metaheuristic for Global Optimization Problems, 2018 IEEE Congress on Evolutionary Computation (CEC), IEEE; 2018, pp. 1–8.
21. Kaveh A, Bakhshpoori T. A new metaheuristic for continuous structural optimization: water evaporation optimization, *Struct Multidisc Optim* 2016; **54**: 23–43.
22. Mirjalili SA, Gandomi AH, Mirjalili SZ, Saremi S, Faris H, Mirjalili SM. Salp swarm algorithm: A bio-inspired optimizer for engineering design problems, *Adv Eng Softw* 2017; **114**: 163–91.
23. Shahrouzi M. Switching teams algorithm for sizing optimization of truss structures, *Int J Optim Civil Eng* 2020; **10**: 365–89.
24. Degertekin SO, Lamberti L, Hayalioglu MS. Heat transfer search algorithm for sizing optimization of truss structures, *Latin American J Solid Struct* 2017; **14**: 373–97.
25. Kaveh A, Akbari H, Hosseini SM. Plasma generation optimization: a new physically-based metaheuristic algorithm for solving constrained optimization problems, *Eng Comput* 2020; **83**: 1554–606.
26. Shahrouzi M, Kaveh A. An efficient derivative-free optimization algorithm inspired by

avian life-saving manoeuvres, *J Comput Sci* 2022; **57**: 101483.
27. Kaveh A, Dadras Eslamlou A. Water strider algorithm: A new metaheuristic and applications, *Struct* 2021; **25**: 520–41.
28. Kaveh A. *Advances in Metaheuristic Algorithms for Optimal Design of Structures*, 3rd ed. Springer Nature Switzerland AG, 2021.
29. Kaveh A, Bakhshpoori T. *Metaheuristics: Outlines, MATLAB Codes and Examples*, Springer Nature Switzerland, 2019.
30. Dorigo M, Stützle T. *Ant Colony Optimization*, London, UK: The MIT press, 2016.
31. Kaveh A, Zolghadr A. A guided modal strain energy based approach for structural damage identification using Tug of War Optimization algorithm, *Amerianc Society Civil Eng* 2017: 1–12.
32. Eberhart R, Kennedy J. New optimizer using particle swarm theory, *Proceedings of the Sixth International Symposium on Micro Machine and Human Science*, 1995, pp. 39–43.
33. INBC: Part-10. *Iranian National Building Code, Part-10: Design of Steel Structures*, 4th ed, Tehran: Roads, Housing and Urban Development of Iran, 2013.
34. Shahrouzi M. Pseudo-random Directional Search: a new heuristic for optimization, *Int J Optim Civil Eng* 2011; **1**: 341–55.
35. INBC: Part-6. *Iranian National Building Code, Part-6: Loading on Structures*, 4th ed. Tehran: Roads, Housing and Urban Development of Iran, 2013.